Robust method for estimating the Lindblad operators of a dissipative quantum process from measurements of the density operator at multiple time points

N. Boulant, T. F. Havel, M. A. Pravia, and D. G. Cory

Department of Nuclear Engineering, MIT, Cambridge, Massachusetts 02139

We present a robust method for quantum process tomography, which yields a set of Lindblad operators that optimally fit the density operators measured at a sequence of time points. The benefits of this method are illustrated using a set of liquid-state nuclear magnetic resonance measurements on a molecule containing two coupled hydrogen nuclei which are sufficient to fully determine its relaxation superoperator. It was found that the complete positivity constraint, which is necessary for the existence of the Lindblad operators, was also essential for obtaining a *robust* fit to the measurements. The general approach taken here promises to be broadly useful in studying dissipative quantum processes in many of the diverse experimental systems currently being developed for quantum-information processing purposes.

I. INTRODUCTION

An important task in designing and building devices capable of quantum-information processing (QIP) is to determine the superoperators that describe the evolution of their component subsystems from experimental measurements. This task is commonly known in QIP as *quantum process tomography* (QPT) [1]. The superoperators obtained from QPT allow one to identify the dominant sources of decoherence and focus development efforts on eliminating them, while precise knowledge of relevant parameters can be used to design quantum error correcting codes and/or decoherence-free subsystems that circumvent their effects [1,2]. Methods have previously been described by which the "superpropagator" $\mathcal{P}$ of a quantum process can be determined [3,4]. Assuming that the process' statistics are stationary and Markovian [5,6], a more complete description may be obtained by determining the corresponding "supergenerator," that is, a time-independent superoperator $\mathcal{G}$ from which the superpropagator at any time t is obtained by solving the differential equation $\dot{\mathcal{P}}(t) = -\mathcal{G}\mathcal{P}(t)$. The formal solution to this equation is $\exp(-\mathcal{G}t)$, where "exp" is the superoperator exponential.

The purpose of this paper is to describe a data fitting procedure by which estimates of a supergenerator can be obtained. This problem is nontrivial because, as in many other data fitting problems, the estimates obtained from the straightforward (e.g., least-squares) fits turn out to be very sensitive to small, even if random, errors in the measured data. In some cases, this may result in a supergenerator that is obviously physically impossible; in others, it may simply result in large errors in the generator despite it yielding a reasonably good fit to the data. Parameter estimation problems with this property are commonly known as *ill-conditioned* [7,8]. The main result of this paper is that, although the problem of estimating a supergenerator from the measurements of the superpropagators at various times is ill-conditioned, this ill-conditioning can be greatly alleviated by incorporating prior knowledge of the solution into the fitting procedure as a constraint. The prior knowledge that

we use here is a very general property of open quantum system dynamics known as *complete positivity*.

Roughly speaking, complete positivity means that if $\mathcal{P}$ is a superoperator that maps a density operator of a system to another density operator, then any extension of the form $\mathcal{I} \otimes \mathcal{P}$ also returns a positive operator, where $\mathcal{I}$ denotes the identity map on an extension of the domain of $\mathcal{P}$. The most general form of a completely positive Markovian master equation for the density operator ρ of a quantum system is known as the Lindblad equation [5,6]. This may be written as

$$\dot{\rho}(t) = -\imath[H,\rho(t)] + \tfrac{1}{2}\sum_{m=1}^{M}\{[L_m\rho(t),L_m^\dagger]+[L_m,\rho(t)L_m^\dagger]\},\tag{1}$$

where $\hbar = 1$, t is time, H is the system's Hamiltonian, L_m are known as Lindblad operators, and $L_m^\dagger$ denote their adjoints. It is easily seen that the Lindblad equation necessarily preserves the trace $\mathrm{tr}(\rho)=1$ of the density matrix, meaning $\mathrm{tr}(\dot{\rho})=0$, and a little harder to show that it also preserves the positive-semidefinite character of the density operator. Proofs that it has the yet-stronger property of complete positivity may be found in Refs. [5,9–11]. The QPT method we describe in this paper relies upon the Lindblad characterization of complete positivity.

The paper is organized as follows. In the first part of the paper we present a computational procedure that fits a completely positive supergenerator to a sequence of estimates of the superpropagators of a quantum process at multiple time points. This procedure initially extracts an estimate of the decoherent part of the supergenerator, without the Hamiltonian commutation superoperator (which is assumed to be available from independent prior measurements). It then refines this initial estimate via a nonlinear least-squares fit to the superpropagators, in which complete positivity is enforced by adding a suitable penalty function to the sum of the squares minimized. Finally, any residual noncompletely positive part of the supergenerator is "filtered" out by a matrix projection technique based on principle component analysis [11,12].

In the second part of the paper, the procedure is validated by using it to determine the natural spin-relaxation superoperator of a molecule containing two coupled spin 1/2 nuclei in the liquid state from a temporal sequence of density operators. These, in turn, were derived by state tomography, meaning a set of nuclear magnetic resonance (NMR) measurements sufficient to determine the density matrix. In the process we confirm the ill-conditioned nature of the problem, and that the complete positivity constraint is needed to obtain a robust estimate of the supergenerator. The final results are used to compute a compatible set of Lindblad operators, but these were difficult to interpret. Hence the Hadamard representation of T_2-relaxation dynamics [13] was used to derive a new set of Lindblad operators that are easier to interpret and explain most of the relaxation dynamics. The information these operators convey agree with theoretical expectations as well as with some additional independent measurements, in support of the accuracy of the results obtained.

II. COMPUTATIONAL PROCEDURE

In this paper we are concerned with an N-dimensional open quantum system ($N<\infty$), the dynamics of which are described by a Markovian master equation of the form [5,6,14]:

$$\frac{d\rho}{dt} = -\iota[H,\rho] - \mathcal{R}(\rho - \rho_{\mathrm{eq}})$$

$$\Leftrightarrow \frac{d\rho_\Delta}{dt} = -\iota\mathcal{H}\rho_\Delta - \mathcal{R}\rho_\Delta. \tag{2}$$

In this equation, $\hbar \equiv 1$, $\rho = \rho(t)$ is the system's density operator, ρ_{eq} this operator at thermal equilibrium, $\rho_\Delta \equiv \rho - \rho_{\mathrm{eq}}$, H is the system's internal Hamiltonian, $\mathcal{H}$ the corresponding commutation superoperator, and $\mathcal{R}$ is the so-called *relaxation superoperator*. The equivalence of the first and second lines follows from the fact that ρ_{eq} is time-independent and proportional to the Boltzmann operator $\exp(-H/k_BT)$, so that it commutes with H.

By choosing a basis for the "Liouville space" of density operators, the equation may be written in matrix form as [11,14,15]

$$\frac{d|\underline{\rho}_\Delta\rangle}{dt} = -(\iota\underline{\mathcal{H}} + \underline{\mathcal{R}})|\underline{\rho}_\Delta\rangle \equiv -\underline{\mathcal{G}}|\underline{\rho}_\Delta\rangle, \tag{3}$$

where the underlines denote the corresponding matrices vs some Liouville space basis and $|\underline{\rho}\rangle$ is the N^2-dimensional column vector obtained by stacking the columns of the density matrix $\underline{\rho}$ on top of each other in left-to-right order [11]. A numerical solution to this equation at any point t in time may be obtained by applying the propagator $\underline{\mathcal{P}}(t)$ to the initial condition $|\underline{\rho}_\Delta(0)\rangle$, where the propagator is obtained by computing the matrix exponential $\underline{\mathcal{P}}(t) = \underline{\exp}(-\underline{\mathcal{G}}t)$ [15,16]. Note that $\underline{\mathcal{H}}$ and $\underline{\mathcal{R}}$ do not commute in general, and that the sum $\underline{\mathcal{G}} \equiv \iota\underline{\mathcal{H}} + \underline{\mathcal{R}}$ will not usually be a normal matrix (one which commutes with its adjoint). This, in turn, greatly reduces the efficiency and stability with which its matrix ex-

ponential can be computed [17] (although this was not an issue in the small problems dealt with here), and we expect it to also significantly complicate the *inverse problem*.

In this section we describe an algorithm for solving this inverse problem, that is, to determine the relaxation superoperator $\mathcal{R}$ from an estimate of the Hamiltonian $\underline{H}$ together with estimates of the propagator $\underline{\mathcal{P}}_m = \underline{\mathcal{P}}(t_m)$ at $M \geq 1$ time points $0 < t_1 < t_2 < \cdots < t_M$. This problem, like many other inverse problems, turns out to be ill-conditioned, meaning that small experimental errors in the estimates of the $\underline{H}$ and $\underline{\mathcal{P}}_m$ may be amplified to surprisingly large, and generally nonphysical, errors in the resulting superoperator $\underline{\mathcal{R}}$ [7]. For example, if one tries to estimate $\underline{\mathcal{R}}$ in the obvious way as

$$\underline{\mathcal{R}} \approx [-\iota\underline{\mathcal{H}} - \underline{\ln}(\underline{\mathcal{P}}_1)]/t_1, \tag{4}$$

one will generally obtain nonsense even if $\underline{\mathcal{H}}$ and $\underline{\mathcal{P}}_1$ are known to machine precision, because of the well-known ambiguity of the matrix logarithm with respect to the addition of independent multiples of $2\iota\pi$ onto its eigenvalues. Using the principal branch of the logarithms will only work if $\mathcal{H}$ is small compared to $\mathcal{R}$, and the only reasonably reliable means of resolving the ambiguities is to utilize additional data and/or prior knowledge of the solution. Even then, a combinatorial search for the right multiples of $2\iota\pi$ may be infeasibly time consuming.

An alternative to the logarithm, which utilizes data at multiple time points and is capable of resolving the ambiguities even when $\mathcal{H}$ is much larger than $\mathcal{R}$, is to estimate the derivative at $t=0$ of

$$\underline{e}^{it\underline{\mathcal{H}}/2}\underline{\mathcal{P}}(t)\underline{e}^{it\underline{\mathcal{H}}/2} = \underline{e}^{-t\underline{\mathcal{R}}} + O(t^2). \tag{5}$$

This derivative is obtained by Richardson extrapolation, using central differencing about $t=0$ over a sequence of time points such that $t_m = 2^{m-1}t_1$ ($m=1,\ldots,M$), according to the well-known procedure [18]:

for m from 1 to M do

$$\underline{\mathcal{D}}_{1,1+M-m} := 2^{m-2}(\underline{e}^{it_m\underline{\mathcal{H}}/2}\underline{\mathcal{P}}_m\underline{e}^{it_m\underline{\mathcal{H}}/2}$$
$$-\underline{e}^{-it_m\underline{\mathcal{H}}/2}\underline{\mathcal{P}}_m^{-1}\underline{e}^{-it_m\underline{\mathcal{H}}/2});$$

for ℓ from 1 to $m-1$ do

$$\underline{\mathcal{D}}_{1+\ell,1+M-m} := \underline{\mathcal{D}}_{\ell,1+M-m}$$
$$+(\underline{\mathcal{D}}_{\ell,1+M-m} - \underline{\mathcal{D}}_{\ell,M-m})/(4^\ell - 1);$$

end do
end do

The inverse $\underline{\mathcal{P}}_m^{-1} = \underline{\mathcal{P}}(-t_m)$ is assured of existing unless long times are used or the errors in the data are large. The method produces an estimate of the derivative at $t=0$ that is accurate up to $O(t_1^{2M})$, and which may be increased by computing the exponential from the highest-order estimate at further interval halvings. The method performs well when the relative errors in the Hamiltonian $\delta \ll 1/(\Delta\nu t_M)$, where $\Delta\nu$ is the range of frequencies present in the Hamiltonian, but it tends to emphasize the errors in $\underline{\mathcal{P}}_1$ rather than averaging over the

errors at all the time points. Hence we do not recommend that it be used alone, but rather as a means of obtaining a good starting point for a nonlinear fit to the data, as will now be described.

This nonlinear fit involves minimization of the sum of squares

$$\chi^2(\underline{\mathcal{R}};\underline{\mathcal{H}},\underline{\mathcal{P}}_1,\ldots,\underline{\mathcal{P}}_M) \equiv \sum_{m=1}^{M} \|\underline{\exp}[-(\imath\underline{\mathcal{H}}+\underline{\mathcal{R}})t_m]-\underline{\mathcal{P}}_m\|_F^2$$

(6)

with respect to $\underline{\mathcal{R}}$, where $\|\cdot\|_F^2$ denotes the squared Frobenius norm (sum of squares of the entries of its matrix argument). Previous results with similar minimization problems indicate that χ^2 will have many local minima [19], making a good starting point that takes the $2\imath\pi$ ambiguities into account absolutely necessary. The derivatives of this function may be obtained via the techniques described in Ref. [16], but the improvements in efficiency to be obtained by their use are likely to be of limited value in practice given that all the resources needed, both experimental and computational, grow rapidly with N (which itself grows exponentially with the number of qubits used in quantum information processing problems). In addition, the quality of the results matters a great deal more than the speed with which they are obtained, and the quality will not generally depend greatly on the accuracy with which the minimum is located.

For these reasons, we have used the Nelder-Mead simplex algorithm [20], as implemented in the MATLAB™ program, for the small (two-qubit) experimental test problem described in the following section. This has the further advantage of being able to avoid local minima better than most gradient-based optimization algorithms. Preliminary numerical studies, however, exhibited the anticipated ill-conditioning with respect to small perturbations in the data, even when $\underline{\mathcal{R}}$ was constrained to be symmetric (implying a unital system which satisfies detailed balance) and positive semidefinite (as required for the existence of a finite fixed point). Therefore, it is necessary to incorporate additional prior information regarding $\underline{\mathcal{R}}$ into the minimization. The information that we have found to be effective is a property of $\underline{\mathcal{R}}$ known as *complete positivity* [5,6,11].

An *intrinsic* definition which does not involve an environment was first given by Kraus [21], and states that a superpropagator $\mathcal{P}$ is completely positive if and only if it can be written as a "Kraus operator sum," namely,

$$\mathcal{P}(\rho) = \sum_{\ell=1}^{N^2} K_\ell \rho K_\ell^\dagger, \qquad (7)$$

where $\rho=\rho^\dagger$ and $K_1,\ldots,K_{N^2}$ all act on the system alone. Another intrinsic definition subsequently given by Choi [22] states that a superpropagator is completely positive if and only if, relative to any basis of the system's Hilbert space, the so-called *Choi matrix* is positive semidefinite [11], namely,

$$\underline{0} \preccurlyeq \underline{\mathcal{C}} \equiv \sum_{i,j=0}^{N-1} \underline{\mathcal{P}(|i\rangle\langle j|)} \otimes (|i\rangle\langle j|) = \sum_{i,j=0}^{N-1} \underline{\mathcal{P}}(|i\rangle|j\rangle)(\langle i|\langle j|).$$

(8)

This equation uses the notation of quantum information processing, in which the ith elementary unit vector is denoted by $|i\rangle$ $(0\leqslant i<N)$, $\underline{\mathcal{P}(|i\rangle\langle j|)}$ is the $N\times N$ matrix of the operator obtained by applying the superpropagator $\mathcal{P}$ to the projection operator given by $|i\rangle\langle j|$ versus our choice of basis, and $\underline{\mathcal{P}}$ is the $N^2\times N^2$ matrix for $\mathcal{P}$ versus the Liouville space basis $|i\rangle|j\rangle$ (as for $\underline{\mathcal{H}}$, etc., above). It can further be shown that the eigenvectors $\underline{k}_\ell$ of the Choi matrix are related to the (matrices of an equivalent set of) Kraus operators by $|\underline{K}_\ell\rangle = \sqrt{\kappa_\ell}\underline{k}_\ell$, where $\kappa_\ell\geqslant0$ are the corresponding eigenvalues and the "ket" $|\underline{K}_\ell\rangle$ again indicates the column vector obtained by stacking the columns of $\underline{K}_\ell$ on top of one another [11].

These results can be used not only to compute a Kraus operator sum from any completely positive superpropagator given as a "supermatrix" acting on the N^2-dimensional Liouville space, but also to "filter" such a supermatrix so as to obtain the supermatrix of the completely positive superpropagator nearest to it, in the sense of minimizing the Frobenius norm of their difference [11]. This is done simply by setting any negative eigenvalues of the Choi matrix to zero, rebuilding it from the remaining eigenvalues and vectors, and converting this reconstructed Choi matrix back to the corresponding supermatrix. Although this generally has a beneficial effect upon the least-squares fits versus χ^2 (as defined above), it is still entirely possible that the sequence of filtered propagators $\mathcal{P}'_m$ will not correspond to a completely positive *Markovian* process, so that no time-independent relaxation superoperator $\mathcal{R}$ can fit it precisely. This, together with the ill-conditioned nature of the problem, implies one will still not usually obtain satisfactory results even after filtering. For this reason we shall now describe how the above characterizations of completely positive superpropagators can be extended to supergenerators.

As indicated in the Introduction, completely positive Markovian processes, or *quantum dynamical semigroups* as they are also known, may be characterized as those with a generator $\mathcal{G}$ that can be written in Lindblad form [5,6,9–11]. On expanding the commutators in Eq. (1), this becomes

$$-\mathcal{G}(\rho) \equiv -\imath[H,\rho] + \tfrac{1}{2}\sum_{m=1}^{N^2} (2L_m\rho L_m^\dagger - L_m^\dagger L_m\rho - \rho L_m^\dagger L_m).$$

(9)

The operators L_m are usually called *Lindblad* operators. It may be seen that the Choi matrix $\underline{\mathcal{C}}$ associated with $-\underline{\mathcal{R}}$ is *never* positive semidefinite, because $\langle\underline{I}|\underline{\mathcal{C}}|\underline{I}\rangle=\mathrm{tr}(-\underline{\mathcal{R}})<0$. Nevertheless, it can be shown that the superpropagator obtained by taking the exponential of any trace-preserving supergenerator $\underline{\mathcal{R}}$ [meaning $\mathrm{tr}(\mathcal{R}(\rho))=\langle\underline{I}|\underline{\mathcal{R}}|\rho\rangle=0$] is completely positive if and only if a certain projection of $\underline{\mathcal{C}}$ is positive semidefinite, namely, $\underline{\mathcal{E}}\,\underline{\mathcal{C}}\,\underline{\mathcal{E}}$, where $\underline{\mathcal{E}}=\underline{I}\otimes\underline{I}-|\underline{I}\rangle\langle\underline{I}|$ [11]. In this case an equivalent system of orthogonal Lindblad operators is determined by $|\underline{L}_m\rangle=\sqrt{\lambda_m}\underline{\ell}_m$, where λ_m
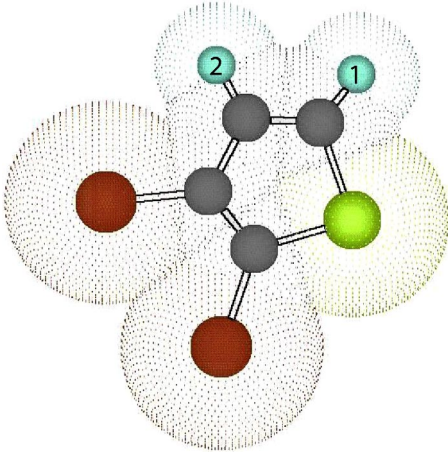
FIG. 1. Molecule of 2,3-dibromothiophene with the two protons labeled 1 and 2. The chemical bonds among the atoms are indicated by double parallel lines, and a transparent "dot-surface" used to indicate their van der Waals radii.

TABLE I. Table of operators (vs Cartesian basis) of the transition basis used for the density and superoperator matrices, the corresponding matrix indices and their coherence orders (see text).

Index	Operator	Order
1	4×4 identity	0
2	σ_z^1	0
3	σ_z^2	0
4	$\sigma_z^1 \sigma_z^2$	0
5	$\sigma_x^1 \sigma_x^2 + \sigma_y^1 \sigma_y^2$	0
6	$\sigma_x^1 \sigma_y^2 - \sigma_y^2 \sigma_x^1$	0
7	σ_x^1	1
8	σ_y^1	1
9	σ_x^2	1
10	σ_y^2	1
11	$\sigma_x^1 \sigma_z^2$	1
12	$\sigma_y^1 \sigma_z^2$	1
13	$\sigma_z^1 \sigma_x^2$	1
14	$\sigma_z^1 \sigma_y^2$	1
15	$\sigma_x^1 \sigma_x^2 - \sigma_y^1 \sigma_y^2$	2
16	$\sigma_x^1 \sigma_y^2 + \sigma_y^1 \sigma_x^2$	2

≥ 0 are the eigenvalues and $\underline{\ell}_m$ the eigenvectors of $\underline{\mathcal{E}}\,\underline{\mathcal{C}}\,\underline{\mathcal{E}}$. In the event that $\underline{\mathcal{E}}\,\underline{\mathcal{C}}\,\underline{\mathcal{E}}$ has negative eigenvalues we can simply set them to zero to obtain a similar but completely positive supergenerator, much as we did with the Kraus operators. Most importantly, however, this characterization of completely positive supergenerators gives us a means of enforcing complete positivity during nonlinear fits to a sequence of propagators at multiple time points.

The following section describes our experience with applying this approach to a sequence of superpropagators obtained from liquid-state NMR data. The complete positivity of the relaxation superoperator was maintained by adding a simple penalty function onto the sum of squares that was minimized by the simplex algorithm, as described above. This penalty function consisted of the sum of the squares of the negative eigenvalues of the corresponding projected Choi matrix. While more rigorous and efficient methods of forcing the projected Choi matrix to be positive semidefinite are certainly possible, this strategy was sufficient to demonstrate the main result of this paper, which is that *the complete positivity constraint greatly alleviates the ill-conditioned nature of such fits.*

III. EXPERIMENTAL VALIDATION

The experiments were carried out on a two-spin-$\frac{1}{2}$ system consisting of the hydrogen atoms in 2,3-dibromothiophene (see Fig. 1) at 300 K dissolved in deuterated acetone, using a Bruker Avance 300 MHz spectrometer. The internal Hamiltonian of this system in a frame rotating at the frequency of the second spin is

$$H \equiv H_{int} = \pi[\nu_1 \sigma_z^1 + (J/2)\sigma^1 \cdot \sigma^2] \qquad (10)$$

where $\nu_1 = 161.63$ Hz is the chemical shift of the first spin, $J = 5.77$ Hz is the coupling between the spins, and $\sigma = [\sigma_x, \sigma_y, \sigma_z]$ are Pauli spin operators.

The "quantum operation" we characterized was just free evolution of the system under its internal Hamiltonian, together with decoherence and relaxation back towards the equilibrium state $\rho_{eq} \sim \sigma_z^1 + \sigma_z^2$. In liquid-state NMR on small organic molecules such as dibromothiophene, this process is mediated primarily by fluctuating dipolar interactions between the two protons as well as with spins neighboring molecules, and since the correlation time for small molecules in room temperature liquids is on the order of picoseconds, the Markovian approximation is certainly valid [14,24]. We add that our sample was not degassed so that the presence of dissolved paramagnetic O_2 shortened the T_1 and T_2 relaxation times considerably.

The experiment consisted of preparing a complete set of orthogonal input states (that is, density matrices), letting each evolve freely for a given time T, and then determining the full output states via quantum state tomography [25,26]. Since only "single quantum" coherences can be directly observed in NMR [14], this involves repeating the experiment several times followed by a different readout pulse sequence each time, until all the entries of the density matrix have been mapped into observable ones. The experiments were carried out at four exponentially spaced times T, as required by the Richardson extrapolation procedure described above, specifically $T = 0.4, 0.8, 1.6$, and 3.2 s.

To describe the density and superoperator matrices, the so-called "transition basis" was used [14]. This Liouville space basis is intermediate between the Cartesian basis and the Zeeman (or polarization and shift operator [14]) basis, in that the basis elements are all Hermitian like those of the Cartesian basis, but like the Zeeman basis they have a well-defined *coherence order*, or difference in total angular momentum along the applied magnetic field B_0 between the two Zeeman states connected by the transition. These basis states are listed in Table I versus the Cartesian basis.

This basis was chosen because the relaxation superoperator $\mathcal{R}$ is expected to have the "Redfield kite" structure in this
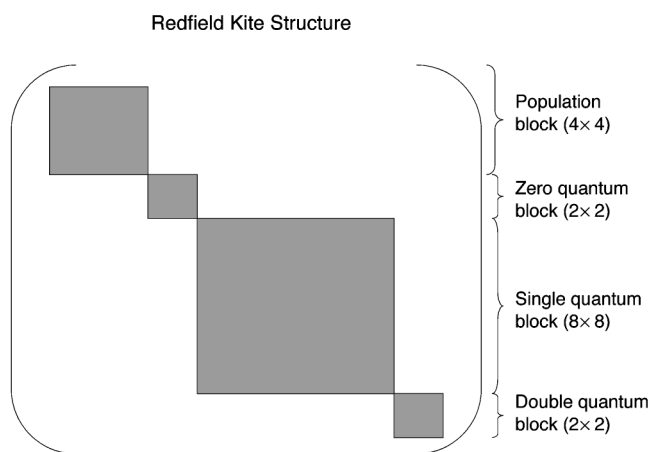
Redfield Kite Structure

FIG. 2. Redfield kite structure of the relaxation superoperator expressed in the transition basis (Table I). The shaded area corresponds to blocks of different coherence order, which are effectively decoupled from each other.

basis [14]. This block-diagonal structure arises because the difference in frequency between transitions of different coherence orders, given that the Zeeman interaction dominates all others, is large enough to average out these other interactions including those responsible for decoherence and relaxation, in effect decoupling the blocks from one another so that no *cross relaxation* occurs between them (see Fig. 2). This so-called "secular approximation" considerably reduces the number of parameters in the superoperator from 256 $=[(2^2)^2]^2$ to $81=3^2+2^2+8^2+2^2$ [since the diagonal (σ_z) basis elements do not cross relax with any nondiagonal elements].

An additional reduction may be obtained by assuming detailed balance: the microscopic reversibility of all cross-relaxation processes. The relaxation superoperator reconstructed from the experimental data was bordered with an initial row and column of zeros to force $\mathcal{R}(I)=0$, because the totally random density matrix $I/4$ neither varies nor contributes to the variations in any of the other transition operators. This may be done provided $\mathcal{R}$ operates on $\rho_\Delta = \rho - \rho_{eq}$, and together with detailed balance it implies that the supermatrix $\underline{\mathcal{R}}$ will be symmetric, reducing the number of parameters to be estimated to only $48=6+3+36+3$.

The result of applying the fitting procedure without the complete positivity constraint to the initial estimate obtained by Richardson extrapolation is shown in Fig. 3(a). It may be seen that the self-relaxation rates did not vary in a systematic fashion with the coherence order and that large cross-relaxation rates were found, neither of which is consistent with the physics of spin relaxation in liquid-state NMR spectroscopy [14]. In addition, this relaxation superoperator implies that spin 1 has a $T_2 \approx 2.3$ s, while spin 2 has a $T_2 \approx 4.6$ s, in disagreement with the independent measurements of T_2 given below.

The fit after adding the complete positivity constraint is shown in Fig. 3(b), again starting from the results of the Richardson extrapolation. It may now be seen that the results do vary systematically with coherence number and that the resulting relaxation superoperator is very nearly diagonal. To

obtain further evidence for the validity of this superoperator, we measured the single-spin T_1 (longitudinal, or σ_z) and T_2 (transverse, or $\sigma_x = \sigma_y$) relaxation rates, using the well-established inversion-recovery and Carr-Purcell-Meiboom-Gill (CPMG) experiments [24]. The results for both spins were $T_1 = 5.6$ s and $T_2 = 2.7$ s, which agree quite well with the values of 5.6 s and 2.6 s obtained from this relaxation superoperator. Although this is obviously a relatively simple relaxation superoperator, it is reasonable to expect that a complete positivity constraint will substantially improve the estimates of more complicated superoperators containing nonzero cross-relaxation rates that cannot be obtained from the standard experiments.

Finally, the cross-relaxation rate between the population terms σ_z^1 and σ_z^2, which is due to the well-known nuclear Overhauser effect (NOE) [27], is essentially zero in Fig. 3(b). This can occur when the overall rotational correlation time of the molecule plus its "solvent-cage" is on the order of 1 ns, but was somewhat unexpected given the small size of 2,3-dibromothiophene. As a result, we carried out the selective inversion recovery experiment that consists of inverting selectively the longitudinal magnetization of one of the two protons and looking at the evolution of the magnetization of the other one while the first relaxes towards thermal equilibrium. The change in longitudinal magnetization of the second proton was measured to be less than 1% of the unperturbed magnetization revealing essentially no NOE effect and providing yet further evidence for the validity of this superoperator. The lack of any appreciable NOE in our sample is somewhat surprising, and implies a rotational correlation time τ_c for dibromothiophene of order $1/\omega_0 \simeq 500$ ps, at which value theory predicts the NOE will vanish [14]. This is somewhat surprising given the modest molecular weight (242 D) of dibromothiophene, the low viscosity of the acetone solvent used, and the value $\tau_c = 4.4$ ps reported in [24] with the solvent carbon disulfide. A much longer correlation time is consistent with the shorter T_1 relaxation time of our sample (5.6 s instead of 47.5 s [24]), although the T_1 was also shortened by the presence of dissolved oxygen in our sample. The correlation time reported in Ref. [24] was derived from a dipole-dipole T_2 of 88 s. Since this is not expected to be affected by dissolved oxygen, a stronger indication of a much longer correlation time may be found in our dipole-dipole $T_2 = 3.4$ s, which is derived from our experimental results in the Appendix. This implies that our $\tau_c \simeq 113.9$ ps, which although still a little short is at least getting close enough to lead to some reduction in the NOE. Such a long correlation time may be rationalized as a "solvent cage" effect due to electric dipole interactions between the solvent and solute in our sample, which is not present in the nonpolar solvent carbon disulfide.

Because of the substantial degeneracy of the diagonal elements with the same coherence order, the superoperator in Fig. 3(b) was also very nearly diagonal in the eigenbasis of the Hamiltonian commutation superoperator $\mathcal{H}$, so that $\mathcal{H}$ and $\mathcal{R}$ very nearly commute. This allowed further estimates to be obtained directly from the superpropagators $\underline{P}_m \approx \underline{\exp}(-\imath \underline{\mathcal{H}} t_m) \underline{\exp}(-\underline{\mathcal{R}} t_m)$, simply by taking the (real) logarithms of the absolute values of their eigenvalues, and
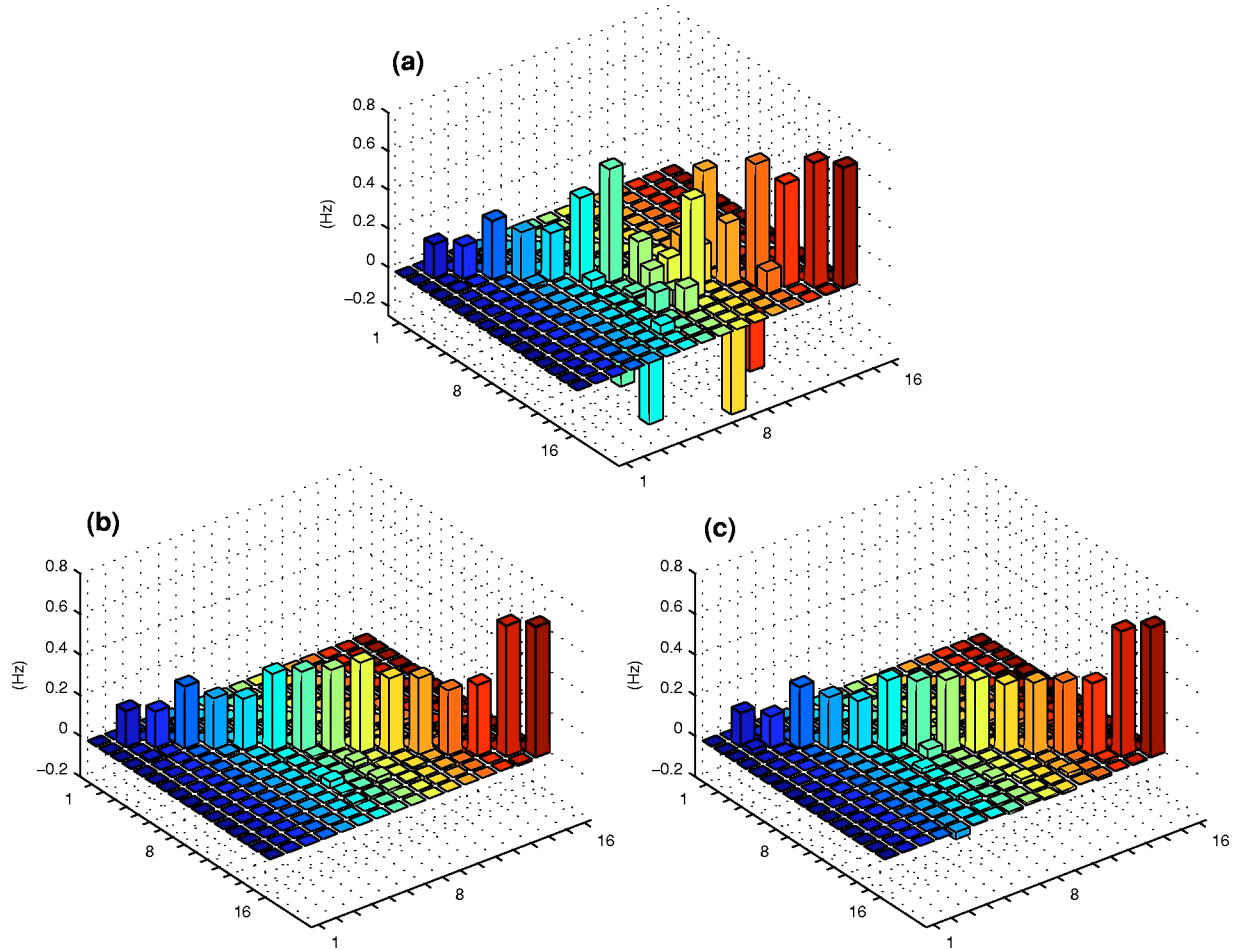
FIG. 3. Three different estimates of the relaxation superoperator of 2,3-dibromothiophene in the transition basis, indexed as indicated in Table I. (a) Relaxation superoperator obtained from a least-squares fit, without the complete positivity constraint, of the exponential $\underline{\exp}[-\iota(\underline{\mathcal{H}}+\underline{\mathcal{R}})t_m]$ to the propagators $\underline{\mathcal{P}}_m$ at the corresponding times ($t_1=0.4, t_2=0.8, t_3=1.6, t_4=3.2$ s) with respect to the symmetric Redfield kite relaxation superoperator matrix $\underline{\mathcal{R}}$, starting from the results of Richardson extrapolation (see text). (b) The relaxation superoperator obtained from a fit to the same data and with the same starting value of $\underline{\mathcal{R}}$, but with the complete positivity constraint included in the fit. (c) The relaxation superoperator obtained by assuming that $\mathcal{H}$ and $\mathcal{R}$ commute, and using the average of the estimates obtained by taking the logarithms of the absolute values of the eigenvalues of the propagators over all four time points as the final estimate (see text).

thereby canceling the phase factors from the Hamiltonian exponential. From Fig. 3(c) we see that the result of averaging these estimates over all four evolution times is very similar to the completely positive estimate in Fig. 3(b) (correlation coefficient 0.80; ratio of squared norm of the difference to that of the average 0.90). We note that the estimate in Fig. 3(c) did not explicitly assume the Redfield kite structure, thereby providing a further consistency check on our results.

IV. INTERPRETATION VIA LINDBLAD AND HADAMARD OPERATORS

In this section we present a system of Lindblad operators, which act on the density operator to give essentially the same derivative as the relaxation superoperator described above (see Fig. 3). As described in the foregoing "Computational Procedure" section, such a system of Lindblad operators may be obtained by diagonalizing the corresponding projected Choi matrix, although it will be seen that a more easily interpreted system was obtained by considering the parts of $\mathcal{R}$

responsible for T_1 and T_2 relaxation separately using the "Hadamard relaxation matrix" formalism [13]. Because these calculations were somewhat involved, however, the details are given in the Appendix. From here on, the relaxation superoperator $\mathcal{R}$ will correspond to the matrix shown in Fig. 3(b).

These representations of relaxation processes are normally applied to the density matrix in the Zeeman basis $\underline{\rho}_\Delta^{Zee}$ (regarded as the computational basis in QIP), which requires converting the supergenerator $\mathcal{R}$ from the transition to the Zeeman basis. This is easily done via a unitary transformation, $\underline{\mathcal{R}}^{Zee} \equiv 2\underline{U} \underline{\mathcal{R}}^{tra} \underline{U}^\dagger$, where $\underline{U}|\underline{\rho}^{tra}\rangle = |\underline{\rho}^{Zee}\rangle$ (the matrix $\underline{U}$ may be derived from Table I; the factor of 2 corrects for a change in norm due to the fact that the transition basis is Hermitian). Although any relaxation superoperator can be modified to act directly on the density operator ρ rather than its difference with the equilibrium density operator $\rho_\Delta = \rho - \rho_{eq}$ (*vide supra*) by taking the right projection $\mathcal{R}(\mathcal{I} - |\underline{\rho}_{eq}\rangle\langle\underline{\mathcal{I}}|)$ [28,29], this makes only a negligible change to

$\mathcal{R}$ since in liquid-state NMR ρ_{eq} differs from the identity I by $\|\rho_{\text{eq}} - I\|_F / \|I\|_F \lesssim 10^{-5}$. In any case, the treatment of T_1 relaxation given in the Appendix was considerably simplified by treating it as a unital (identity preserving) process acting on ρ_Δ.

As described following Eq. (9), a complete system of Lindblad operators may be obtained by diagonalizing the projected Choi matrix

$$\underline{\mathcal{E}}\,\underline{\mathcal{C}}\,\underline{\mathcal{E}} = \underline{V}\,\underline{\Lambda}\,\underline{V}^\dagger, \tag{11}$$

where it is assumed that the eigenvalues have been ordered such that $\lambda_m \geq \lambda_{m+1}$ for $m = 1, \ldots, N^2 - 1$, and defining the Lindblad matrices such that for all $\lambda_m > 0$:

$$|\underline{L}_m\rangle = \sqrt{\lambda_m}\underline{V}|m\rangle. \tag{12}$$

This gave rise to a total of 11 Lindblad operators, the phases of which were chosen so as to make them as nearly Hermitian as possible. Once this was done, all 11 operators were within 2% of being Hermitian.

The relative contributions of these Lindblad operators to the overall relaxation of the spins can be quantified by the squared Frobenius norms $\|\underline{L}_m\|_F^2 = \lambda_m$. This calculation shows that about 35% of the mean-square noise resided in the first Lindblad operator, namely,

$$\underline{L}_1 \approx 0.346(\underline{\sigma}_z^1 + \underline{\sigma}_z^2) + 0.025\underline{\sigma}_z^1\underline{\sigma}_z^2, \tag{13}$$

which represents strongly correlated dephasing with a T_2 for both spins of ~ 4.2 s [13], much as expected. The next four largest Lindblads together contributed, roughly equally, another 43% to the total mean-square noise, but were considerably more difficult to interpret

$$\underline{L}_2 \approx -0.013\underline{\sigma}_x^1 - 0.045\underline{\sigma}_y^1 - 0.153\underline{\sigma}_x^2 - 0.061\underline{\sigma}_y^2 + 0.150\underline{\sigma}_x^1\underline{\sigma}_z^2$$
$$- 0.039\underline{\sigma}_y^1\underline{\sigma}_z^2 + 0.111\underline{\sigma}_z^1\underline{\sigma}_x^2 + 0.106\underline{\sigma}_z^1\underline{\sigma}_y^2,$$

$$\underline{L}_3 \approx +0.046\underline{\sigma}_z^1 - 0.026\underline{\sigma}_z^2 - 0.057\underline{\sigma}_x^1\underline{\sigma}_y^2 - 0.266\underline{\sigma}_z^1\underline{\sigma}_z^2, \tag{14}$$

$$\underline{L}_4 \approx -0.024\underline{\sigma}_x^1 - 0.006\underline{\sigma}_y^1 - 0.081\underline{\sigma}_x^2 - 0.077\underline{\sigma}_y^2 - 0.155\underline{\sigma}_x^1\underline{\sigma}_z^2$$
$$- 0.193\underline{\sigma}_y^1\underline{\sigma}_z^2 + 0.002\underline{\sigma}_z^1\underline{\sigma}_x^2 - 0.012\underline{\sigma}_z^1\underline{\sigma}_y^2,$$

$$\underline{L}_5 \approx -0.017\underline{\sigma}_x^1 - 0.060\underline{\sigma}_y^1 - 0.071\underline{\sigma}_x^2 - 0.090\underline{\sigma}_y^2 + 0.090\underline{\sigma}_x^1\underline{\sigma}_z^2$$
$$- 0.001\underline{\sigma}_y^1\underline{\sigma}_z^2 - 0.183\underline{\sigma}_z^1\underline{\sigma}_x^2 - 0.118\underline{\sigma}_z^1\underline{\sigma}_y^2.$$

It can be shown that L_3 contributes about 0.15 s^{-1} to the decay rates of the single-quantum coherences (single-spin flips), bringing down the decay time $T_2 \approx 2.6$ s and, save for some small cross terms in the single quantum block, rather little else.

The superoperators corresponding to each of the remaining nine Lindblads separately all contained significant cross terms between the populations and the zero or double quantum coherences, in violation of the secular approximation [14]. Only on summing over all of them do these nonphysical cross terms cancel out, leaving a largely diagonal relax-

ation superoperator behind: the ratio of the mean-square value of the off-diagonal entries of $\mathcal{R}$ to that of the diagonal entries was 1.3% in the transition basis and 3.8% in the Zeeman; the latter dropped to 1.8% on excluding the block corresponding to T_1 relaxation of the populations (*vide infra*). The nonphysical nature of most of the Lindblads is clearly an artifact of the way that our procedure for calculating them forces them to be orthogonal and minimal in number. In order to physically interpret the dominant relaxation processes, we therefore focus our attention first on T_1 relaxation among the populations (diagonal entries of the density matrix in the Zeeman basis), along with the associated nonadiabatic T_2 relaxation, and then try to account for the remaining T_2 relaxation via simple adiabatic, albeit correlated, processes.

The calculations given in the Appendix gave four Hermitian Lindblad operators, which describe the T_1 relaxation of the first spin,

$$L_{T_1}^{x1} = \sqrt{0.1532}\tfrac{1}{2}\sigma_x^1, \quad L_{T_1}^{y1} = \sqrt{0.1532}\tfrac{1}{2}\sigma_y^1,$$

$$L_{T_1}^{xz} = \sqrt{0.1532}\tfrac{1}{2}\sigma_x^1\sigma_z^2, \quad L_{T_1}^{yz} = \sqrt{0.1532}\tfrac{1}{2}\sigma_y^1\sigma_z^2, \tag{15}$$

and similarly for the second spin,

$$L_{T_1}^{x2} = \sqrt{0.1528}\tfrac{1}{2}\sigma_x^2, \quad L_{T_1}^{y2} = \sqrt{0.1528}\tfrac{1}{2}\sigma_y^2,$$

$$L_{T_1}^{zx} = \sqrt{0.1528}\tfrac{1}{2}\sigma_z^1\sigma_x^2, \quad L_{T_1}^{zy} = \sqrt{0.1528}\tfrac{1}{2}\sigma_z^1\sigma_y^2. \tag{16}$$

In addition, near degeneracy of the (1,4) and (2,3) rates in the relaxation superoperator in the Zeeman basis can be used to combine the associated Lindblad operators into four multiple-quantum T_1 Lindblad operators based on the average rate:

$$L_{T_1}^{xx} = \sqrt{0.0252}\tfrac{1}{2}\sigma_x^1\sigma_x^2, \quad L_{T_1}^{xy} = \sqrt{0.0252}\tfrac{1}{2}\sigma_x^1\sigma_y^2,$$

$$L_{T_1}^{yx} = \sqrt{0.0252}\tfrac{1}{2}\sigma_y^1\sigma_x^2, \quad L_{T_1}^{yy} = \sqrt{0.0252}\tfrac{1}{2}\sigma_y^1\sigma_y^2. \tag{17}$$

By working through some examples, it may be seen that the sum of the Lindbladian superoperators for each of the three sets of four Lindblad operators above also causes all the off-diagonal entries of ρ_Δ^{Zee} to decay with the rate constant $1/(2T_1)$. This corresponds to *nonadiabatic* T_2 relaxation. Therefore, we subtracted this nonadiabatic T_2 contribution to get the adiabatic T_2 contribution to $\mathcal{R}$ and derived the following three Lindblad operators from it, using the Hadamard operator formalism [13]:

$$L_{T_2}^{\text{ad1}} = \sqrt{0.9560}\frac{1}{\sqrt{8}}(\sigma_z^1 + \sigma_z^2), \quad L_{T_2}^{\text{ad2}} = \sqrt{0.1721}\frac{1}{\sqrt{8}}(\sigma_z^1 - \sigma_z^2),$$

$$L_{T_2}^{\text{ad3}} = \sqrt{0.2931}\tfrac{1}{2}\sigma_z^1\sigma_z^2. \tag{18}$$

These correspond to totally correlated, totally anticorrelated, and pure single-quantum T_2 relaxation, respectively [13]. Although the Hadamard product formalism gave a simpler description with a clearer physical interpretation, it left a small discrepancy between the complete relaxation superoperator reconstructed from the new Linblad operators above and the

completely positive relaxation superoperator $\mathcal{R}^{\text{Zee}}$ obtained by fitting to the experimental superpropagators [Fig. 3(b)]. The matrix of the relaxation superoperator reconstructed from the new Lindblad operators above, $\mathcal{R}_{\text{new}}^{\text{Zee}}$, was obtained by taking the 4×4 matrices for the T_1 and adiabatic T_2 relaxation, i.e., $\underline{R}_{T_1}^{\text{Zee}}$ and $\underline{R}_{T_2}^{\text{Zee}}$ in the Appendix, and distributing their entries at the corresponding locations of the 16 $\times$ 16 matrix $\mathcal{R}_{\text{new}}^{\text{Zee}}$ while setting all its other entries to zero. The discrepancy was then quantified by computing the relative difference between the superoperators, namely,

$$\frac{\|\underline{\mathcal{R}}^{\text{Zee}} - \underline{\mathcal{R}}_{\text{new}}^{\text{Zee}}\|_F}{\|\underline{\mathcal{R}}^{\text{Zee}}\|_F}. \tag{19}$$

This gave a value of 6.3%, which is roughly comparable to the errors in the measurements of the density operators ($\sim 5\%$), indicating that the simplifying assumptions made in deriving the new Lindblad operators are able to account for the experiments to within the measurement errors. These assumptions included a lack of any correlations in the underlying T_1 processes as well as the absence of cross relaxation in the adiabatic T_2 processes, and are in accord with what is expected in the NMR experiments on small molecules in the liquid state [14].

V. CONCLUSION

In this paper, we have demonstrated a robust procedure by which one can derive a set of Lindblad operators that collectively account for a Markovian quantum process, with a minimum of prior assumptions regarding the nature of the process beyond the physical necessity of complete positivity. This procedure should be widely useful in studies of dissipative quantum processes and in designing and testing new quantum information processing devices. In the Appendix,

we have further shown how one can use the simpler and more intuitive "Hadamard operator" formalism to extract the physical "noise generators" of the system from its full relaxation superoperator. We believe this two-step process is illustrative of how quantum process tomography on many distinct kinds of physical systems should be done.

APPENDIX

In this appendix we derive the physical "noise generators" operative in 2,3-dibromothiophene from the full relaxation superoperator matrix shown in Fig. 3(b), after converting it from the transition to the Zeeman basis. First, the T_1 submatrix was extracted and, assuming that the random fields responsible are uncorrelated at the two spins, used to derive the corresponding T_1 Linblad operators. The nonadiabatic T_2 relaxation rates are then subtracted from the diagonal entries of the relaxation superoperator matrix in the Zeeman basis, and the result arranged as a "Hadamard relaxation matrix" [13] (*vide infra*). Finally, this was decomposed to yield a totally correlated, a totally anticorrelated, and a pure single quantum Lindblad operator which collectively described the adiabatic T_2 relaxation.

The populations block of the relaxation superoperator corresponds to indices 1–4 in the transition basis (see Table I.) and the nonzero entries of $|I\rangle\langle I|$ in the Zeeman basis. The values obtained from the completely positive least-squares fit shown in Fig. 3(b) are

$$\underline{R}_{T_1}^{\text{tra}} = \begin{bmatrix} 0.0000 & 0.0000 & 0.0000 & 0.0000 \\ 0.0000 & 0.1780 & -0.0002 & 0.0089 \\ 0.0000 & -0.0002 & 0.1784 & -0.0097 \\ 0.0000 & 0.0089 & -0.0097 & 0.3061 \end{bmatrix} \leftrightarrow \begin{bmatrix} 0.3301 & -0.1435 & -0.1617 & -0.0249 \\ -0.1435 & 0.3129 & -0.0254 & -0.1440 \\ -0.1617 & -0.0254 & 0.3500 & -0.1630 \\ -0.0249 & -0.1440 & -0.1629 & 0.3319 \end{bmatrix} = \underline{R}_{T_1}^{\text{Zee}} \tag{A1}$$

with columns labeled iden, $\underline{\sigma}_z^1$, $\underline{\sigma}_z^2$, $\underline{\sigma}_z^1\underline{\sigma}_z^2$ (left) and $|\uparrow\uparrow\rangle$, $|\uparrow\downarrow\rangle$, $|\downarrow\uparrow\rangle$, $|\downarrow\downarrow\rangle$ (right).

in the transition (left) as well as the Zeeman (right) bases. The matrices $\underline{R}_{T_1}^{\text{tra}}$ and $\underline{R}_{T_1}^{\text{Zee}}$ are related by the *Hadamard transform* $\underline{W}$ [13,23],

$$\underline{W} \equiv \frac{1}{2}\begin{bmatrix} 1 & 1 & 1 & 1 \\ 1 & 1 & -1 & -1 \\ 1 & -1 & 1 & -1 \\ 1 & -1 & -1 & 1 \end{bmatrix}, \tag{A2}$$

that is,

$$2\underline{W}\,\underline{R}_{T_1}^{\text{Zee}}\underline{W} = \underline{R}_{T_1}^{\text{tra}} \leftrightarrow \underline{R}_{T_1}^{\text{Zee}} = \tfrac{1}{2}\underline{W}\,\underline{R}_{T_1}^{\text{tra}}\underline{W}, \tag{A3}$$

since $\underline{W}^2 = \underline{I}$. In the absence of cross correlation, symmetry considerations imply that $\underline{R}_{T_1}^{\text{Zee}}$ should be centrosymmetric [24,27], and hence we shall use the symmetrized version $\frac{1}{2}(\underline{R}_{T_1}^{\text{Zee}} + \underline{\sigma}_x^1\underline{\sigma}_x^2\underline{R}_{T_1}^{\text{Zee}}\underline{\sigma}_x^1\underline{\sigma}_x^2)$ and its Hadamard transform in the following, which are

$$\underline{R}_{T_1}^{\text{tra}} = \begin{bmatrix} 0.0000 & -0.0000 & -0.0000 & 0.0000 \\ 0.0000 & 0.1780 & -0.0002 & 0.0000 \\ 0.0000 & -0.0002 & 0.1784 & 0.0000 \\ 0.0000 & 0.0000 & 0.0000 & 0.3061 \end{bmatrix}$$

$$\leftrightarrow \begin{bmatrix} 0.3310 & -0.1532 & -0.1528 & -0.0249 \\ -0.1532 & 0.3315 & -0.0254 & -0.1528 \\ -0.1528 & -0.0254 & 0.3315 & -0.1532 \\ -0.0249 & -0.1528 & -0.1532 & 0.3310 \end{bmatrix}$$

$$= \underline{R}_{T_1}^{\text{Zee}}. \tag{A4}$$

As noted in the main paper, the T_1 of both spins is ~ 5.6 s, while the NOE rate (connecting σ_z^1 and σ_z^2 in the transition basis) is negligibly small (-0.0002).

The entries of $-\underline{R}_{T_1}^{\text{Zee}}$ are equal to the diagonal entries of the Choi matrix $\underline{\mathcal{C}}$ of $-\underline{\mathcal{R}}^{\text{Zee}}$, and the off-diagonal entries of $\underline{R}_{T_1}^{\text{Zee}}$ are the *only* non-negligible entries in their respective rows and columns of $\underline{\mathcal{C}}$. Therefore, they are eigenvalues of the Choi matrix as well as its projection $\underline{\mathcal{E}}\,\underline{\mathcal{C}}\,\underline{\mathcal{E}}$, and their corresponding eigenvectors are elementary unit vectors $|k\rangle|j\rangle$ relative to the Zeeman basis. It follows that the Lindblad operator for the (j,k)th off-diagonal entry of $\underline{R}_{T_1}^{\text{Zee}}$ may be written as $\underline{L}_{T_1}^{jk} \equiv (-\langle j|\underline{R}_{T_1}^{\text{Zee}}|k\rangle)^{1/2}|k\rangle\langle j|$, and its contribution to $\dot{\rho}_\Delta^{\text{Zee}}$ is given by

$$\underline{L}_{T_1}^{jk}(\underline{\rho}_\Delta^{\text{Zee}}) \equiv -\langle j|\underline{R}_{T_1}^{\text{Zee}}|k\rangle(|k\rangle\langle j|\underline{\rho}_\Delta^{\text{Zee}}|j\rangle\langle k| - \tfrac{1}{2}|j\rangle\langle j|\underline{\rho}_\Delta^{\text{Zee}}$$
$$- \tfrac{1}{2}\underline{\rho}_\Delta^{\text{Zee}}|j\rangle\langle j|). \tag{A5}$$

The symmetry of $\underline{R}_{T_1}^{\text{Zee}}$ implies that the eigenvalues of $\underline{\mathcal{C}}$ corresponding to single spin flips (the so-called single-quantum coherences) are fourfold degenerate, and hence we can replace their elementary unit eigenvectors by arbitrary unitary linear combinations thereof. For example, the four Lindblad operators which describe the T_1 relaxation of the first spin may be replaced by the Hermitian operators:

$$\underline{L}_{T_1}^{x1} = \sqrt{0.1532}\,\tfrac{1}{2}(|2\rangle\langle 0| + |0\rangle\langle 2| + |3\rangle\langle 1| + |1\rangle\langle 3|)$$
$$= \sqrt{0.1532}\,\tfrac{1}{2}\underline{\sigma}_x^1,$$

$$\underline{L}_{T_1}^{y1} = \sqrt{0.1532}\,\frac{i}{2}(|2\rangle\langle 0| - |0\rangle\langle 2| + |3\rangle\langle 1| - |1\rangle\langle 3|)$$
$$= \sqrt{0.1532}\,\tfrac{1}{2}\underline{\sigma}_y^1,$$

$$\underline{L}_{T_1}^{xz} = \sqrt{0.1532}\,\tfrac{1}{2}(|2\rangle\langle 0| + |0\rangle\langle 2| - |3\rangle\langle 1| - |1\rangle\langle 3|)$$
$$= \sqrt{0.1532}\,\tfrac{1}{2}\underline{\sigma}_x^1\underline{\sigma}_z^2,$$

$$\underline{L}_{T_1}^{yz} = \sqrt{0.1532}\,\frac{i}{2}(|2\rangle\langle 0| - |0\rangle\langle 2| - |3\rangle\langle 1| + |1\rangle\langle 3|)$$
$$= \sqrt{0.1532}\,\tfrac{1}{2}\underline{\sigma}_y^1\underline{\sigma}_z^2. \tag{A6}$$

In a similar fashion, we may take those describing T_1 relaxation of the second spin to be

$$\underline{L}_{T_1}^{1x} = \sqrt{0.1528}\,\tfrac{1}{2}\underline{\sigma}_x^2, \quad \underline{L}_{T_1}^{1y} = \sqrt{0.1528}\,\tfrac{1}{2}\underline{\sigma}_y^2,$$

$$\underline{L}_{T_1}^{zx} = \sqrt{0.1528}\,\tfrac{1}{2}\underline{\sigma}_z^1\underline{\sigma}_x^2, \quad \underline{L}_{T_1}^{zy} = \sqrt{0.1528}\,\tfrac{1}{2}\underline{\sigma}_z^1\underline{\sigma}_y^2. \tag{A7}$$

In addition, the near degeneracy of the (1,4) and (2,3) rates can be used to combine the associated Lindblad operators into four multiple-quantum T_1 Lindblad operators based on the average rate:

$$\underline{L}_{T_1}^{xx} = \sqrt{0.0252}\,\tfrac{1}{2}\underline{\sigma}_x^1\underline{\sigma}_x^2, \quad \underline{L}_{T_1}^{xy} = \sqrt{0.0252}\,\tfrac{1}{2}\underline{\sigma}_x^1\underline{\sigma}_y^2,$$

$$\underline{L}_{T_1}^{yx} = \sqrt{0.0252}\,\tfrac{1}{2}\underline{\sigma}_y^1\underline{\sigma}_x^2, \quad \underline{L}_{T_1}^{yy} = \sqrt{0.0252}\,\tfrac{1}{2}\underline{\sigma}_y^1\underline{\sigma}_y^2. \tag{A8}$$

By working through some examples, it may be seen that the sum of the Lindbladian superoperators for each of the three sets of four Lindblad operators above also causes all the off-diagonal entries of ρ_Δ^{Zee} to decay with the rate constant $1/(2T_1)$. This corresponds to *nonadiabatic* T_2 relaxation. Because $\underline{R}_{T_1}^{\text{Zee}}$ does not act on its off-diagonal entries, it may also be seen that if one takes the Lindblad operators $(\langle k|\underline{R}_{T_1}^{\text{Zee}}|k\rangle)^{1/2}|k\rangle\langle k|$ of the four diagonal entries of $\underline{R}_{T_1}^{\text{Zee}}$ and *subtracts* their superoperators from those for the off-diagonal entries, this must exactly cancel the nonadiabatic T_2 decay. Formally, however, the negative of a Lindbladian superoperator is not a Lindbladian superoperator, and in any case we do not really want to cancel the nonadiabatic T_2, since it actually occurs. In order to avoid accounting for the nonadiabatic T_2 twice, it is nevertheless necessary to write down a set of Lindblad operators for it alone, without any T_1 relaxation. Once again, on using the near equality of the diagonal entries of $\underline{R}_{T_1}^{\text{Zee}}$ to replace them by their average and taking suitable unitary linear combinations of the diagonal Lindblads $|j\rangle\langle j|$, we obtain

$$\underline{L}_{T_1}^{\text{na0}} = \sqrt{0.3312}\,\tfrac{1}{2}I, \quad \underline{L}_{T_1}^{\text{na1}} = \sqrt{0.3312}\,\tfrac{1}{2}\underline{\sigma}_z^1,$$

$$\underline{L}_{T_1}^{\text{na2}} = \sqrt{0.3312}\,\tfrac{1}{2}\underline{\sigma}_z^2, \quad \underline{L}_{T_1}^{\text{na3}} = \sqrt{0.3312}\,\tfrac{1}{2}\underline{\sigma}_z^1\underline{\sigma}_z^2. \tag{A9}$$

The Lindbladian superoperator of the first of these is obviously $\underline{L}_{T_1}^{\text{na0}}(\rho_\Delta) = \underline{0}$, and so need not be considered further.

We now turn our attention to the diagonal entries of the 16×16 Zeeman relaxation superoperator $\underline{\mathcal{R}}^{\text{Zee}}$, which we shall arrange in a 4×4 matrix of relaxation rate constants of the corresponding entries of the density matrix ρ_Δ^{Zee}. It can be shown that the 4×4 matrix

$$R_{\underline{\text{diag}}}^{\text{Zee}} \equiv \begin{bmatrix} \langle 00|\underline{\mathcal{R}}^{\text{Zee}}|00\rangle & \langle 01|\underline{\mathcal{R}}^{\text{Zee}}|01\rangle & \langle 02|\underline{\mathcal{R}}^{\text{Zee}}|02\rangle & \langle 03|\underline{\mathcal{R}}^{\text{Zee}}|03\rangle \\ \langle 10|\underline{\mathcal{R}}^{\text{Zee}}|10\rangle & \langle 11|\underline{\mathcal{R}}^{\text{Zee}}|11\rangle & \langle 12|\underline{\mathcal{R}}^{\text{Zee}}|12\rangle & \langle 13|\underline{\mathcal{R}}^{\text{Zee}}|13\rangle \\ \langle 20|\underline{\mathcal{R}}^{\text{Zee}}|20\rangle & \langle 21|\underline{\mathcal{R}}^{\text{Zee}}|21\rangle & \langle 22|\underline{\mathcal{R}}^{\text{Zee}}|22\rangle & \langle 23|\underline{\mathcal{R}}^{\text{Zee}}|23\rangle \\ \langle 30|\underline{\mathcal{R}}^{\text{Zee}}|30\rangle & \langle 31|\underline{\mathcal{R}}^{\text{Zee}}|31\rangle & \langle 32|\underline{\mathcal{R}}^{\text{Zee}}|32\rangle & \langle 33|\underline{\mathcal{R}}^{\text{Zee}}|33\rangle \end{bmatrix} \tag{A10}$$

is also a symmetric submatrix of the Choi matrix $\underline{\mathcal{C}}$ associated with $\underline{\mathcal{R}}^{\text{Zee}}$ (up to sign), specifically

$$-R_{\underline{\text{diag}}}^{\text{Zee}} = \begin{bmatrix} \langle 00|\underline{\mathcal{C}}|00\rangle & \langle 00|\underline{\mathcal{C}}|11\rangle & \langle 00|\underline{\mathcal{C}}|22\rangle & \langle 00|\underline{\mathcal{C}}|33\rangle \\ \langle 11|\underline{\mathcal{C}}|00\rangle & \langle 11|\underline{\mathcal{C}}|11\rangle & \langle 11|\underline{\mathcal{C}}|22\rangle & \langle 11|\underline{\mathcal{C}}|33\rangle \\ \langle 22|\underline{\mathcal{C}}|00\rangle & \langle 22|\underline{\mathcal{C}}|11\rangle & \langle 22|\underline{\mathcal{C}}|22\rangle & \langle 22|\underline{\mathcal{C}}|33\rangle \\ \langle 33|\underline{\mathcal{C}}|00\rangle & \langle 33|\underline{\mathcal{C}}|11\rangle & \langle 33|\underline{\mathcal{C}}|22\rangle & \langle 33|\underline{\mathcal{C}}|33\rangle \end{bmatrix}. \tag{A11}$$

The diagonal of $\underline{R}_{\text{diag}}^{\text{Zee}}$ is thus the same as the diagonal of $\underline{R}_{T_1}^{\text{Zee}}$. Since we have already found a set of Lindblad operators that fully account for the effects of $\underline{R}_{T_1}^{\text{Zee}}$ on $\rho_{\Delta}^{\text{Zee}}$, we will now focus our attention on its off-diagonal entries by defining a new matrix $\underline{R}_{T_2}^{\text{Zee}}$, which is same as $\underline{R}_{\text{diag}}^{\text{Zee}}$ save for its four diagonal entries, which are set to zero as indicated below:

$$\underline{R}_{T_2}^{\text{Zee}} \equiv \underline{R}_{\text{diag}}^{\text{Zee}} - \underline{\text{Diag}}(\langle kk|\underline{\mathcal{R}}^{\text{Zee}}|kk\rangle | k=0,\ldots,3). \tag{A12}$$

As implied by our notation, $\underline{R}_{T_2}^{\text{Zee}}$ contains all the information regarding T_2 relaxation processes that is contained in our full, but *diagonal*, relaxation superoperator $\mathcal{R}^{\text{Zee}}$, and in a considerably more compact and easily understood form. Unlike $\underline{R}_{T_1}^{\text{Zee}}$, which acts on the column vector $\underline{\text{diag}}(\rho_{\Delta}^{\text{Zee}})$ of diagonal entries by matrix multiplication, $\underline{R}_{T_2}^{\text{Zee}}$ acts on $\rho_{\Delta}^{\text{Zee}}$ simply by taking the products of all corresponding pairs of entries, one from each matrix, just as these entries are multiplied together in the full matrix-vector product $\underline{\mathcal{R}}^{\text{Zee}}|\rho_{\Delta}^{\text{Zee}}\rangle$. This "entrywise" matrix multiplication, commonly known as the *Hadamard product* [15], has already been shown to be a powerful means of describing "simple" T_2 relaxation processes [13] (that is, processes not involving cross relaxation). The Hadamard product will be denoted in the following:

$$\dot{\rho}_{\Delta}^{\text{Zee}} = -\underline{R}_{T_2}^{\text{Zee}} \odot \rho_{\Delta}^{\text{Zee}} \equiv -[\langle j|\rho_{\Delta}^{\text{Zee}}|k\rangle\langle j|\underline{R}_{T_2}^{\text{Zee}}|k\rangle]_{j,k=0}^{3}. \tag{A13}$$

Another important property of the matrix $\underline{R}_{T_2}^{\text{Zee}}$ is that, since the overall projected Choi matrix $\underline{\mathcal{E}}\,\underline{\mathcal{C}}\,\underline{\mathcal{E}}$ must be positive semidefinite, the same is true of the projection of $-\underline{R}_{T_2}^{\text{Zee}}$, and the 4×4 block of the 16×16 projection matrix $\underline{\mathcal{E}}$ that acts on $-\underline{R}_{T_2}^{\text{Zee}}$ is

$$\underline{E} \equiv \underline{I} - \frac{1}{4}\underline{1}\,\underline{1}^{\top} = \frac{1}{4}\begin{bmatrix} 3 & -1 & -1 & -1 \\ -1 & 3 & -1 & -1 \\ -1 & -1 & 3 & -1 \\ -1 & -1 & -1 & 3 \end{bmatrix}, \tag{A14}$$

where $\underline{1}$ denotes a column vector of four 1's. Moreover, the Lindblad operators for T_2 relaxation may be extracted directly from $-\underline{E}\,\underline{R}_{T_2}^{\text{Zee}}\underline{E}$ without reference to the full superoperator's projected Choi matrix.

To see how this can be done, we first observe that given any two diagonal matrices $\underline{A}$ and $\underline{C}$ (assumed here to equal in dimension) with column vectors of diagonal entries $\underline{a} = \underline{\text{diag}}(\underline{A})$ and $\underline{c} = \underline{\text{diag}}(\underline{C})$, respectively, we have

$$\underline{A}\,\underline{B}\,\underline{C} = (\underline{A}\,\underline{1}\,\underline{1}^{\top}\underline{C})\odot\underline{B} = (\underline{a}\,\underline{c}^{\top})\odot\underline{B} \tag{A15}$$

for any other (square but not necessarily diagonal) matrix $\underline{B}$ of equal dimension. It follows that the action on a density operator ρ of any Lindblad operator L, with respect to a basis wherein its matrix $\underline{L}$ is real and diagonal, can be expressed in terms of Hadamard products as

$$\underline{L}(\rho) \equiv \underline{L}\,\rho\,\underline{L} - \tfrac{1}{2}\underline{L}^2\rho - \tfrac{1}{2}\rho\,\underline{L}^2 = (\underline{L}\,\underline{1}\,\underline{1}^{\top}\underline{L} - \tfrac{1}{2}\underline{L}^2\underline{1}\,\underline{1}^{\top} \\ - \tfrac{1}{2}\underline{1}\,\underline{1}^{\top}\underline{L}^2)\odot\rho \equiv -\underline{R}_L\odot\rho, \tag{A16}$$

where $\underline{R}_L$ is called a *Hadamard relaxation matrix* for L. If multiple diagonal Lindblad operators act simultaneously, the net Hadamard relaxation matrix is of course the sum of those associated with the individual Lindblads.

Next, let us use the Lindblad operators for nonadiabatic T_2 relaxation given in Eq. (A9) above, to illustrate how we can go the other way, that is, derive these Lindblad operators from the corresponding Hadamard relaxation matrix. If we let $\underline{\ell}_{T_2}^{\text{nai}} \equiv \underline{\text{diag}}(\underline{L}_{T_2}^{\text{nai}})$ be the column vectors formed from the real diagonal entries of these Lindblad matrices and observe that their Hadamard squares $\underline{\ell}_{T_2}^{\text{nai}}\odot\underline{\ell}_{T_2}^{\text{nai}} = 0.3312\frac{1}{4}\underline{1}$ for $i = 1,2,3$, then Eq. (A15) shows that the nonadiabatic T_2 Hadamard relaxation matrix may be written as

$$-\underline{R}_{T_2}^{\mathrm{na}} \equiv \underline{\ell}_{T_2}^{\mathrm{na1}}(\underline{\ell}_{T_2}^{\mathrm{na1}})^\top + \underline{\ell}_{T_2}^{\mathrm{na2}}(\underline{\ell}_{T_2}^{\mathrm{na1}})^\top + \underline{\ell}_{T_2}^{\mathrm{na1}}(\underline{\ell}_{T_2}^{\mathrm{na1}})^\top$$

$$-\tfrac{1}{2}(\underline{\ell}_{T_2}^{\mathrm{na1}} \odot \underline{\ell}_{T_2}^{\mathrm{na1}} + \underline{\ell}_{T_2}^{\mathrm{na2}} \odot \underline{\ell}_{T_2}^{\mathrm{na2}} + \underline{\ell}_{T_2}^{\mathrm{na3}} \odot \underline{\ell}_{T_2}^{\mathrm{na3}})\underline{1}^\top$$

$$-\tfrac{1}{2}\underline{1}(\underline{\ell}_{T_2}^{\mathrm{na1}} \odot \underline{\ell}_{T_2}^{\mathrm{na1}} + \underline{\ell}_{T_2}^{\mathrm{na2}} \odot \underline{\ell}_{T_2}^{\mathrm{na2}} + \underline{\ell}_{T_2}^{\mathrm{na3}} \odot \underline{\ell}_{T_2}^{\mathrm{na3}})^\top$$

$$=\frac{0.3312}{4}\left(\begin{bmatrix}1\\1\\-1\\-1\end{bmatrix}\begin{bmatrix}1\\-1\\1\\-1\end{bmatrix}^T + \begin{bmatrix}1\\-1\\1\\-1\end{bmatrix}\begin{bmatrix}1\\1\\-1\\-1\end{bmatrix}^T\right.$$

$$\left.+\begin{bmatrix}1\\-1\\-1\\1\end{bmatrix}\begin{bmatrix}1\\1\\1\\1\end{bmatrix}^T\right)$$

$$-\frac{0.3312}{8}\left(\begin{bmatrix}1\\1\\1\\1\end{bmatrix} + \begin{bmatrix}1\\1\\1\\1\end{bmatrix} + \begin{bmatrix}1\\1\\1\\1\end{bmatrix}\right)\begin{bmatrix}1\\-1\\-1\\1\end{bmatrix}^T$$

$$-\frac{0.3312}{8}\begin{bmatrix}1\\1\\1\\1\end{bmatrix}\left([1\ 1\ 1\ 1] + [1\ 1\ 1\ 1] + [1\ 1\ 1\ 1]\right)$$

$$= 0.3312\,(\underline{E} - \tfrac{3}{4}\underline{1}\,\underline{1}^\top)$$

$$=-0.3312\begin{bmatrix}0&1&1&1\\1&0&1&1\\1&1&0&1\\1&1&1&0\end{bmatrix}. \tag{A17}$$

Noting that $\underline{E}^2 = \underline{E}$ and that the row and column sums of $\underline{E}$ are zero, it may be seen that the projection $-\underline{E}\,\underline{R}_{T_2}^{\mathrm{na}}\underline{E}$ simply removes the last two terms involving the Hadamard squares from the above, which are proportional to $\underline{1}\,\underline{1}^\top$, leaving only $-\underline{E}\,\underline{R}_{T_2}^{\mathrm{na}}\underline{E} = 0.3312\underline{E}$ behind. Because the vectors $\underline{\ell}_{T_2}^{\mathrm{na}i}$ are mutually orthogonal and all their squared norms are $\|\underline{\ell}_{T_2}^{\mathrm{na}i}\|^2 = 0.3312$, upon normalization they actually become eigenvectors of $\underline{E}$ that are associated with its one nonzero, but triply degenerate, eigenvalue of unity.

From this we see that the nonzero entries of the diagonal Lindblad matrices $\underline{L}_{T_2}^{\mathrm{na}i}$ are the entries of the eigenvectors of $-\underline{E}\,\underline{R}_{T_2}^{\mathrm{na}}\underline{E}$ times the square roots of their respective eigenval-

ues, much as general Lindblad matrices may be obtained from the eigenvalues and eigenvectors of the projected Choi matrix $\underline{\mathcal{E}}\,\underline{\mathcal{C}}\,\underline{\mathcal{E}}$. The numerical values of the entries of $\underline{R}_{T_2}^{\mathrm{Zee}}$, as extracted from the experimental superoperator in Fig. 3, are

$$\underline{R}_{T_2}^{\mathrm{Zee}} = \begin{bmatrix} 0 & 0.7890 & 0.7757 & 1.2872 \\ 0.7890 & 0 & 0.5033 & 0.7426 \\ 0.7757 & 0.5033 & 0 & 0.7283 \\ 1.2872 & 0.7426 & 0.7283 & 0 \end{bmatrix}\,\mathrm{s}^{-1}. \tag{A18}$$

It is easily seen that $\underline{R}_{T_2}^{\mathrm{Zee}}$, like $\underline{R}_{T_1}^{\mathrm{Zee}}$, must be centrosymmetric, and if we likewise symmetrize and subtract the above nonadiabatic T_2 Hadamard relaxation matrix, we get

$$\underline{R}_{T_2}^{\mathrm{ad}} \equiv \underline{R}_{T_2}^{\mathrm{Zee}} - \underline{R}_{T_2}^{\mathrm{na}} = \begin{bmatrix} 0 & 0.4274 & 0.4279 & 0.9560 \\ 0.4274 & 0 & 0.1721 & 0.4279 \\ 0.4279 & 0.1721 & 0 & 0.4274 \\ 0.9560 & 0.4279 & 0.4274 & 0 \end{bmatrix}. \tag{A19}$$

The nonzero eigenvalues and associated eigenvectors of $-\underline{E}\,\underline{R}_{T_2}^{\mathrm{ad}}\underline{E}$ are (to within 1%)

$$\left(0.9560, \frac{1}{\sqrt{2}}\begin{bmatrix}1\\0\\0\\-1\end{bmatrix}\right), \quad \left(0.2913, \tfrac{1}{2}\begin{bmatrix}1\\-1\\-1\\1\end{bmatrix}\right),$$

$$\left(0.1721, \frac{1}{\sqrt{2}}\begin{bmatrix}0\\1\\-1\\0\end{bmatrix}\right), \tag{A20}$$

which correspond to a system of three Lindblad operators for the adiabatic T_2 relaxation, namely

$$\underline{L}_{T_2}^{\mathrm{ad1}} = \sqrt{0.9560}\,\frac{1}{\sqrt{8}}(\underline{\sigma}_z^1 + \underline{\sigma}_z^2), \quad \underline{L}_{T_2}^{\mathrm{ad2}} = \sqrt{0.1721}\,\frac{1}{\sqrt{8}}(\underline{\sigma}_z^1 - \underline{\sigma}_z^2),$$

$$\underline{L}_{T_2}^{\mathrm{ad3}} = \sqrt{0.2931}\,\tfrac{1}{2}\,\underline{\sigma}_z^1\underline{\sigma}_z^2. \tag{A21}$$

These correspond to totally correlated, totally anticorrelated, and pure single-quantum, i.e. dipolar, T_2 relaxation, respectively [13].

---

[1] M.A. Nielsen and I.L. Chuang, *Quantum Computation and Quantum Information* (Cambridge University Press, Cambridge, 2001).

[2] *The Physics of Quantum Information*, edited by D. Bouwmeester, A. Ekert, and A. Zeilinger (Springer-Verlag, Berlin, 2000).

[3] A.M. Childs, I.L. Chuang, and D.W. Leung, Phys. Rev. A **64**, 012314 (2001).

[4] A. Fujiwara, Phys. Rev. A **63**, 042304 (2001).

[5] R. Alicki and M. Fannes, *Quantum Dynamical Systems* (Ox-

ford University Press, Oxford, 2001).

[6] U. Weiss, *Quantum Dissipative Systems*, 2nd ed. (World Scientific, London, 1999).

[7] P.J. Rousseeuw and A.M. Leroy, *Robust Regression and Outlier Detection* (Wiley, New York, 1987).

[8] A. Tarantola, *Inverse Problem Theory* (Elsevier Science, Amsterdam, 1987).

[9] G. Lindblad, Commun. Math. Phys. **48**, 119 (1976).

[10] V. Gorini, A. Kossakowski, and E.C.G. Sudarshan, J. Math. Phys. **17**, 821 (1976).

[11] T.F. Havel, J. Math. Phys. **44**, 534 (2003).

[12] I.T. Jollife, *Principal Component Analysis* (Springer-Verlag, Berlin, 1986).

[13] T.F. Havel, Y. Sharf, L. Viola, and D.G. Cory, Phys. Lett. A **280**, 282 (2001).

[14] R.R. Ernst, G. Bodenhausen, and A. Wokaun, *Principles of Nuclear Magnetic Resonance in One and Two Dimensions* (Oxford University Press, Oxford, 1994).

[15] R.A. Horn and C.R. Johnson, *Matrix Analysis* (Cambridge University Press, Cambridge, 1985).

[16] I. Najfeld and T.F. Havel, Adv. Appl. Math. **16**, 321 (1995).

[17] C.B. Moler and C.F. van Loan, SIAM Rev. **45**, 3 (2003).

[18] G. Dahlquist and A. Björck, *Numerical Methods* [translated by N. Anderson] (Prentice-Hall, New York, 1974), Secs. 7.2.2.

[19] I. Najfeld, K.T. Dayie, G. Wagner, and T.F. Havel, J. Magn. Reson. **124**, 372 (1997).

[20] J.A. Nelder and R. Mead, Comput. J. (UK) **7**, 308 (1965).

[21] K. Kraus, Ann. Phys **64**, 311 (1971).

[22] M.D. Choi, Linear Algebr. Appl. **10**, 285 (1975).

[23] C.H. Tseng, S. Somaroo, Y. Sharf, E. Knill, R. Laflamme, T.F. Havel, and D.G. Cory, Phys. Rev. A **62**, 032309 (2000).

[24] R. Freeman, S. Wittekoek, and R.R. Ernst, J. Chem. Phys. **52**, 3 (1970).

[25] I.L. Chuang, N. Gershenfeld, M. Kubinec, and D. Leung, Proc. R. Soc. London, Ser. A **454**, 447 (1998).

[26] T.F. Havel, D.G. Cory, S. Lloyd, N. Boulant, E.M. Fortunato, M.A. Pravia, G. Teklemariam, Y.S. Weinstein, A. Bhattacharyya, and J. Hou, Am. J. Phys. **70**, 345 (2002).

[27] I. Solomon, Phys. Rev. **99**, 559 (1955).

[28] T.O. Levante, and R.R. Ernst, Chem. Phys. Lett. **241**, 73 (1995).

[29] R. Ghose, Concepts Magn. Reson. **12**, 152 (2000).